Microfluid Nanofluid (2012) 13:665–674
DOI 10.1007/s10404-012-0977-8

RESEARCH PAPER

Synthesis of magnetic hydrogel microparticles for bioassays and tweezer manipulation in microwells

Su Kyung Suh · Stephen C. Chapin · T. Alan Hatton · Patrick S. Doyle

Received: 27 January 2012 / Accepted: 27 March 2012 / Published online: 10 April 2012

Abstract We report new methods for the synthesis and efficient manipulation of magnetic hydrogel microparticles. Through the development of a high-pH rinsing scheme, we achieve a simple and flexible synthesis strategy for the generation of geometrically and chemically complex magnetic microgels, eliminating the need for perfusion streams and other features that limit production rates and particle complexity. We further demonstrate the ability to combine magnetic functionality with both coding and target capture motifs within the same barcoded particle for enhanced applications in microRNA detection. We use a magnetic tweezer to assist in the positioning of particles in substrate-patterned microwells, and also for selective retrieval of particles. The magnetic particle manipulations and the substrate-mediated patterning techniques described in this work hold great potential for the development of a versatile platform for nanoliter-scale reactions with multifunctional hydrogel microparticles.

Keywords Magnetic particles · MicroRNA assays · Magnetic tweezer · Microwells

1 Introduction

Magnetic particles have enhanced performance and simplified workflow in separation (Miltenyi et al. 1990; Bucak et al. 2003), catalysis (Stevens et al. 2005), and biotechnology processes (Pankhurst et al. 2003; Mornet et al. 2004) since the particles can be manipulated using external magnetic fields and also bear chemical or biological functionality. Within the field of microfluidics, multifunctional magnetic particles have been used for mixing (Jung et al. 2011), display (Yin et al. 2011), separation (Pamme and Manz 2004), encoding (Lee et al. 2010), and immunoassays (Choi et al. 2001; Peyman et al. 2009). Many of these assays take advantage of field-assembled spatial structures or movement of magnetic particles under application of a magnetic field. For example, spherical magnetic particles assemble to form roughly equally spaced chains aligned with a homogeneous magnetic field. This field-assisted patterning of magnetic particles has been used for DNA separation (Doyle et al. 2002), cell enrichment (Saliba et al. 2010), and protein digestion (Slovakova et al. 2005), by providing colloidal lattices with tunable spacing within a microfluidic system. In addition, three-dimensional clusters of magnetic gels have been created on patterned magnets to study cellular structures (Xu et al. 2011). Magnetic forces can be used not only for the assembly of microparticles, but also for the retrieval of particles from previously built structures. For example, cells grown on magnetic microrafts can be released from the patterned substrates and collected with magnets for sorting and subsequent single-cell studies (Gunn et al. 2010).

We previously reported the combination of magnetic materials and graphically encoded hydrogel particles which we synthesized with stop-flow lithography (SFL) (Bong et al. 2010). Such particles can serve as a versatile suspension-array platform for the high-performance, multiplexed detection of a range of biomolecules (Pregibon et al. 2007). In multiplex assays, where multiple targets are simultaneously quantified in a single sample, each particle

Electronic supplementary material The online version of this article (doi:10.1007/s10404-012-0977-8) contains supplementary material, which is available to authorized users.

S. K. Suh · S. C. Chapin · T. A. Hatton · P. S. Doyle (✉)
Massachusetts Institute of Technology, 77 Massachusetts Ave, Cambridge, MA 02139, USA
e-mail: pdoyle@mit.edu

contains one or more spatially separated probe regions and a unique graphical code region used to identify those probe species on that particle. The encoded particles have been used for sensitive, multiplexed quantitation of DNA (Pregibon et al. 2007), microRNA (miRNA) (Chapin et al. 2011), and proteins (Appleyard et al. 2011; Srinivas et al. 2011), with readout in static-imaging or flow-based systems (Chapin et al. 2009). In particular, our miRNA assays utilize not only hybridization of nucleic acids to probes embedded in the particles, but also enzymatic reaction within the substrate and subsequent binding of a protein reporter. These assays require non-fouling, porous substrates functionalized with DNA probes that are accessible for target capture and subsequent enzymatic manipulation.

Diagnostic tools capable of handling small sample volumes are important as most clinical samples are very limited and precious. To address this concern, researchers have used engineered devices such as substrate-patterned microwells to provide a dramatic improvement in assay sensitivity and thus more efficient use of sample (Lindström and Andersson-Svahn 2010; Love et al. 2006). Unfortunately, microwells are not well suited for reagent exchange due to practical limitations in liquid dispensing (Lindström and Andersson-Svahn 2010). The use of particle-based biosensors may help overcome this shortcoming; the deposition of particles into patterned microwells can provide a simple means to achieve robust spatial control, small-volume reaction, and ease of transport. However, the combination of microwells and particle-based biosensors has not been studied extensively due to difficulties in achieving uniform particle distribution and the lack of a means for single-particle manipulation. In this situation, multifunctional magnetic particles could be used to provide precise control and manipulation, but have been challenging to make in an efficient manner.

We previously demonstrated the synthesis and use of magnetic, barcoded hydrogel particles. While the addition of magnetic material to these particles simplified their manipulation and processing, their synthesis was greatly complicated by the need for a perfusion stream, with flow perpendicular to the monomer stream required to eliminate unincorporated magnetic beads that could foul the particles during collection (Bong et al. 2010). An alternate approach to creating magnetic particles is two-step polymerization: after a magnetic region is made using one monomer, a new monomer is introduced and a region containing another chemistry is formed around it (Lee et al. 2010). Beyond lithographic methods, other means to creating multifunctional magnetic particles face their own set of challenges. Two-region Janus magnetic microparticles synthesized using two-phase microfluidic systems require precise viscosity matching between phases (Seiffert et al. 2010; Yuet et al. 2010) or the use of external magnetic fields during polymerization (Dyab et al. 2009; Kim et al. 2010). These requirements restrict the incorporation of magnetic material to certain regions of the particles and limit their chemical complexity.

In this work, we present a new framework for the creation and use of magnetic barcoded particles in substrate-patterned microwells. To simplify the synthesis of magnetic bead-embedded gel particles, we developed a pH-enhanced washing scheme that allows for the removal of unincorporated magnetic material from the surface of the particle in a simple post-synthesis rinse. Although rinsing is carried out in high-pH solutions, we demonstrate that particles synthesized with magnetic code and probe regions maintain their chemical and biological functionality for decoding and miRNA detection. We also demonstrate uniform patterning of the magnetic gel particles in microwells and the selective collection and manipulation of individual particles. In addition to the flexibility afforded by magnetic patterning, the use of microwells also provides a nanoliter-scale volume that can serve as a reaction chamber for particle-based assays.

2 Experimental methods

2.1 Materials

Polymeric particles were made from poly(ethylene glycol) (700) diacrylate (PEG-DA 700, Sigma-Aldrich) and 2-hydroxy-2-methylpropiophenone (Darocur 1173, Sigma-Aldrich) initiator. In pre-polymer solutions, we added poly(ethylene glycol) (200) (PEG 200, Sigma-Aldrich) to obtain the desired solubility of Darocur and fluid viscosity. We used 800-nm diameter carboxylate-modified magnetic bead solutions (Seradyn Inc., carboxylate-modified, 5 % solids) for magnetic functionalization. Tergitol NP-10 (Sigma-Aldrich) or Tween-20 (Sigma-Aldrich) was used at 0.05 % (v/v) to prevent particle loss due to sticking on pipette tips or tubes. Tris–EDTA (TE) buffer (10 mM tris(hydroxymethyl)-aminomethane, 1 mM ethylenediaminetetraacetic acid, pH 8.0) was purchased from Rockland Immunochemicals. Oligonucleotide probe for miR-145 (5Acryd/GAT ATA TTT TAA GGG ATT CCT GGG AAA ACT GGA C/3InvdT) was purchased from IDT with an acrydite modification on the 5′ end (for covalent incorporation into the gel matrix) and mixed into the probe pre-polymer to give a final concentration of 50 μM. New England Buffer #2 (NEB2), ATP, and T4 DNA ligase were purchased from New England Biolabs. A universal labeling adapter (IDT) and streptavidin-r-phycoerythrin fluorophore (SA-PE, Invitrogen) were used to report binding events for miRNA assays, as described elsewhere (Chapin et al. 2011).

2.2 Microfluidic devices

Microfluidic channels for SFL were fabricated using standard soft-lithography techniques. Polydimethylsiloxane (PDMS, Sylgard 184, Dow Corning) in a 10:1 base-to-curing agent ratio was molded on a patterned silicon wafer (SU-8 photoresist, Microchem), then cured in an oven at 65 °C for 2 h. Holes for connections to the inlets and outlet were punched with an 18-gauge luer stub adapter. Glass slides were coated with PDMS and partially cured at 65 °C for 22 min. The clean patterned PDMS was assembled with the PDMS-coated glass and then placed in the oven for 45 min. The prepared microfluidic channel was then connected with inlets that were made from pipette tips (ART 10 Reach and ART 200, Molecular BioProducts, Inc) and outlet aluminum tubing (1/16″, K&S) for collecting particles after synthesis. For particle synthesis, the devices were mounted on an inverted microscope (Axiovert 200, Zeiss).

2.3 Stop-flow-lithography setup

We created hydrogel particles in microfluidic devices when flow was stopped. The formed particles were then moved out of the polymerization area via the pressure-driven flow of fresh monomer solutions. Pulsed flow was operated using automated control scripts for the generation of stop-polymerization-flow cycles, alternating the pressure at all four inlets simultaneously from 0 to 3 psi. The relative widths of the inlet streams were controlled by opening needle valves on a custom-built pressure manifold (Bong et al. 2011). A microscope-mounted UV source (Lumen 200, Prior Scientific, 100 % setting) initiated polymerization reactions (75 ms exposure time). Photomasks were placed in the field-stop slot of the microscope, and the desired excitation spectrum was selected using a UV filter (11000v2, Chroma). UV intensity with the 20× objective of the inverted microscope was 3,400 mW/cm^2, as measured by a UV power meter (Accu-Cal 30, Dymax). The composition of each pre-polymer stream used in this work is summarized in Table 1 and the process is shown schematically in Figure S1.

2.4 Washing scheme

To remove unincorporated magnetic beads, we used high-pH rinse solutions. Particles were washed three times with 1 M NaOH aqueous solution and 0.005 % (v/v) Tergitol (to prevent sticking of hydrogel particles in pipette tips or Eppendorf tube). To separate unincorporated magnetic beads from hydrogel particles, centrifugation was performed for 10 s. Then, the particles were rinsed with deionized water with 0.005 % (v/v) Tergitol three times to decrease pH. For miRNA detection, the particles were suspended and stored in TET (1× TE with 0.05 % (v/v) Tween-20).

2.5 miRNA incubation experiments

All incubations were carried out in 50 µl volumes of TET in 0.65 ml Eppendorf tubes at a final NaCl concentration of 350 mM. Synthetic miR-145 RNA target sequences were diluted in 1× TE such that the addition of 0.5 µl of target solution to the incubation tube introduced 500 amol of target. A previously prepared mix of four types of particles (~12.5 of each type per µl TET) was thoroughly vortexed for 1 min, and 4 µl was introduced to each incubation tube. Incubation with target was carried out at 55 °C for 90 min in a thermomixer (Quantifoil Rio) with a mixing speed of 1,500 rpm. After hybridization with target, the particles were washed three times with a solution of 500 µl TET containing 50 mM NaCl (R50). The supernatant resulting from centrifugal separation was manually removed from the tube. Following the protocol for a ligation-based labeling scheme described elsewhere (Chapin et al. 2011), the 50 µl of solution at the bottom of the tube was preserved after the third rinse, and 245 µl of a previously prepared ligation mastermix (100 µl 10× NEB2, 900 µl TET, 250 nM ATP, 40 nM biotinylated universal adapter sequence, and 800 U/ml T4 DNA ligase) was added to the tube. The mixture was placed in a shaker (Multi-therm) at 21.5 °C for 30 min with a mixing speed of 1,500 rpm. After ligation of the biotinylated universal adapters to the captured targets, the particles were rinsed three times with R50. SA-PE (1 mg/ml) was diluted 1:50 in TET and added

Table 1 Composition of pre-polymer solution in volume %

	PEG-DA 700 (%)	Darocur 1173 (%)	PEG 200 (%)	1× TE (%)	Rhodamine B (%)	Magnetic solution (%)	DNA (µM)	Food coloring (%)
Code	35	5	20	39.85	0.15	N/A	N/A	N/A
Magnetic code	35	5	N/A	18.35	0.15	41.5	N/A	N/A
Probe	18	4.5	36	41.5	N/A	N/A	50	N/A
Magnetic probe	18	4.5	36	N/A	N/A	41.5	50	N/A
Inert	35	5	30	28	N/A	N/A	N/A	2

to the incubation mixture to provide a final dilution of 1:500. Samples were incubated at 21.5 °C at 1,500 rpm for 45 min. After another three-rinse cycle with R50, particles were rinsed once in 500 µl of PTET (5× TE with 25 % (v/v) PEG 400 and 0.05 % Tween-20). Prior to use, all PTET was sonicated for 5 min to eliminate aggregations of polymer. For fluorescence analysis, particles were either imaged individually with an Andor CCD camera or with a microfluidic, high-speed flow-through scanning system (Chapin et al. 2009, 2011).

2.6 Microwell experiments

Wells ($L \times W \times H = 300 \times 100 \times 113$ µm) were fabricated using standard soft-lithography techniques. PDMS was molded on a patterned silicon wafer, and then cured in an oven at 65 °C for 2 h. After removing the PDMS from the wafer, 20 µl of TET was dropped onto the molded wells and distributed with a pipette tip so that the solution could wet the bottom of the wells. Next, 5 µl of particle solution (one magnetic particle/µl) was dropped onto the wetted surface. Using a hand magnet (KS), particles were rotated to align with the long dimension of the rectangular array of wells and translated across the surface to begin the filling process. To facilitate loading via sedimentation, particles were translated slowly and the angle between the PDMS surface and the hand magnet was $\sim 45^{\circ}$. After all particles had been placed in wells ($\sim$2–3 min), five additional particles were deposited and the process was repeated until the desired occupancy had been reached. More TET solution was gently added every 10 min to prevent the wells and surfaces from drying.

2.7 Magnetic tweezer experiment

The magnetic tweezer device used in this work was originally developed by Lammerding (2004). The core was made of high-magnetic-permeability iron (CMI-C, CMI Specialty Products, Bristol, CT, USA) machined to a sharp tip with a width of 200 µm. Then, it was subsequently annealed according to the manufacturer's specifications. The geometry of the sharp tip creates high magnetic field gradients and thus exerts large forces on magnetic particles. The core metal is wrapped with AWG 19 copper magnet wire over a length of 7.2 cm, producing a wire turn density of $\sim$4,200 m^{-1}. By fitting the tweezer into a manual micromanipulator (MX110, Siskiyou, Grants Pass, OR, USA), the instrument was placed beside an inverted microscope (Axiovert 40 CFL, Carl Zeiss AG, Oberkochen, Germany). The wires were connected to a DC power supply (GPS-2303, GWInstek, Taipei, Taiwan) and the magnetic tweezer was operated with a current of $I = 0.15$ A (Rich et al. 2011). During manipulation, the average distance from the magnetic particles to the tweezer was $\sim$150 µm. As particles were collected from the wells using vertical forces, the magnetic tweezer was rotated 90° to measure the relevant force. Magnetic beads with a diameter of 780 nm (0.1 % v/v) were suspended in a glycerol (80 % v/v) and water (20 % v/v) solution with viscosity of 86 cP (Cheng 2008) and exposed to the rotated tweezer. Movies of magnetic beads were captured by a CCD camera at 30 frames per second.

3 Results and discussion

3.1 High-pH rinsing scheme

Figure 1d shows the magnetic barcoded hydrogel particles synthesized using SFL. Particle morphology is dictated by the shape of the features on the transparency mask placed in the path of the UV light, while chemical functionality is determined by the arrangement of fluid inlets in the microfluidic channel. Two inlets were used in this synthesis, creating particles with two distinct regions, one of which contained magnetic material embedded within the polymer matrix. Because the magnetic bead size (800 nm) is much larger than the typical pore size of our particles (5 nm), the beads are physically entrapped within the hydrogel particles. From Fig. 1d, it can be seen that the internal features of the magnetic barcode remain sharp and well defined, demonstrating that the magnetic beads do not significantly reduce the resolution of the SFL process. Graphical codes were defined by the UV masks used during particle synthesis, which had varying sizes for the internal barcode features. The codes "0", "1", "2", and "3" were created via incorporation of holes in the particle (unpolymerized regions) of area of 12×0, 12×15, 12×27.5, and 12×40 µm^2, respectively.

After synthesis, particles are collected in a mixture of unreacted monomer, magnetic beads, and buffer. To prevent magnetic beads from attaching to the surface of the hydrogel particles in this mixture, we developed a method to remove the magnetic beads that were not incorporated in the hydrogel particle matrix via rinsing with a high-pH solution. We used carboxylated magnetic beads because they are dispersed easily in PEG-DA solutions. This is because the carboxylated bead surfaces are deprotonated in high-pH solutions, causing the beads to electrostatically repel one another. Well-dispersed magnetic beads are more easily removed from hydrogel surfaces than are aggregated beads. Furthermore, the hydrogel particles have characteristic sizes on the scale of 100 µm, while the magnetic beads have a characteristic size <1 µm. As a result, a short centrifugation of 10 s can be used to effectively separate hydrogel particles (which sediment) from magnetic beads (which remain in the supernatant).

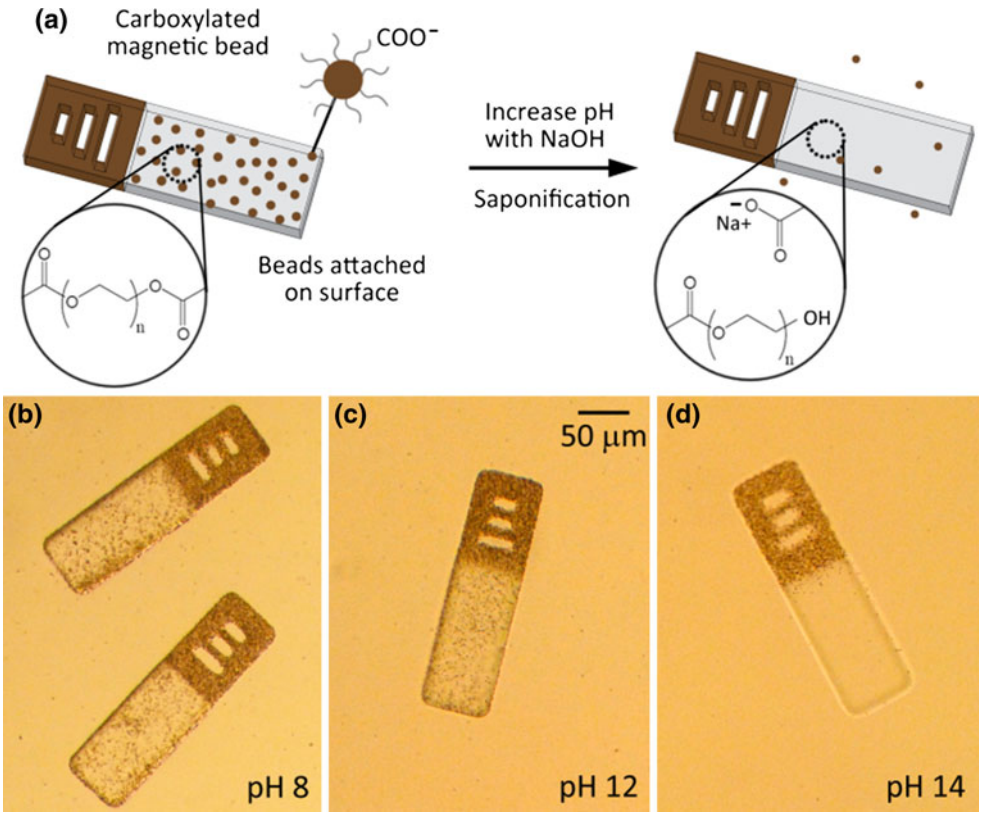

Fig. 1 Demonstration of pH-enhanced rinsing. **a** Schematic of polymer saponification with high pH. The high-pH solution decomposes ester groups to carboxyl and alcohol groups. **b–d** Optical images of magnetic barcoded particles after rinsing with pH 8, 12, and 14 solutions, respectively. The *scale bar* is 50 µm

A range of pHs was tested for the rinsing procedure. Higher pHs are more effective in removing the magnetic beads on the hydrogel particles. While the particles imaged after washing with pH 8 and 12 solutions still have magnetic beads on their surface, those rinsed with pH 14 show clean surfaces as shown in Fig. 1. We note that all of the solutions used have a higher pH than the pK_a of COOH (Fessenden et al. 1998). This implies that the attachment of beads on the hydrogel surfaces is due to an ion–dipole interaction between hydrogels and beads rather than beads with other beads. As ester groups like those present in the hydrogel network can be broken with high pH and increased temperature, it is likely that some of the esters in the cross-linked PEG-DA network are hydrolyzed during high-pH rinsing, as shown in Fig. 1a. This process of saponification produces carboxyl and alcohol groups from the broken esters, which then repel the magnetic beads bound at the gel surface. This electrostatic repulsion facilitates the removal of magnetic beads from hydrogel particles in low ionic strength solutions. This mechanism of saponification has been further corroborated by an additional experiment in which we observed complete decomposition of hydrogel particles exposed to 3 M NaOH at 65 °C for 30 min. However, in the case of rinsing, only a small degree of decomposition occurs, as we expose particles to pH 14 for only about 1 min at room temperature. This insight into the effect of high pH on the PEG-based particles enables us not only to create clean hydrogel particle surfaces, but may also allow for control over the hydrogel pore size by varying the incubation time and temperature in such alkaline solutions.

3.2 Biological functionality of magnetic barcoded particles

To ensure that full particle functionality was retained after the rinse process, we prepared particles designed to detect miR-145, a clinically relevant miRNA target known to be dysregulated in a variety of diseases. We chose miRNA assays for this proof of concept because it utilizes not only hybridization of nucleic acids to probes embedded in the particles, but also enzymatic reaction within the substrate and subsequent binding of a protein reporter. Three types of particles were used in this experiment: control, non-magnetic particles (with barcode 103), particles with a magnetic code region (123), and particles with magnetic code and probe regions (113). After particles were exposed to sample solution containing target and then rinsed with a low-salt buffer, we used T4 DNA ligase to attach a universal biotinylated oligonucleotide adapter to the 3′ end of those targets captured on gel-embedded probes. Then, after another low-salt rinse to remove un-ligated adapter, SA-PE

was introduced to fluorescently label bound-target complexes, as described in Fig. 2a. The particles were imaged using a fluorescence microscope, as shown in Fig. 2b–d. Captured target is indicated by fluorescent signal in the probe region. To simulate a full high-throughput assay, particles were also scanned at high speed using our previously developed flow-through system, and the results for the mean signal over 10–15 particles of each type are presented in Fig. 2e; (Chapin et al. 2009, 2011). While the control particles have slightly higher integrated signals, the pH-treated particles still show a strong signal with excellent particle-to-particle reproducibility. This suggests that the high-pH rinsing scheme does not degrade or release the DNA probes to a degree that would substantially decrease the performance of particles for miRNA detection.

We also observe signal reduction in the code regions that bear magnetic materials, though code features remain mechanically stable in high-speed scanning flows and can still be readily identified. Due to reduced UV penetration through magnetic bead containing pre-polymer during synthesis, the thickness of magnetic regions is smaller than that of non-magnetic regions (Suh et al. 2011). For coding regions covalently functionalized with rhodamine-acrylate, this leads to a reduction in the loading of fluorophore and thus lower fluorescent signal arising from the barcode during analysis. This can easily be corrected by simply increasing the concentration of rhodamine-acrylate in the code pre-polymer. Regarding the magnetic probe regions investigated in this work, the miRNA hybridization events take place predominantly at the surface of the hydrogel (due to relatively faster reaction with probe than diffusion through the gel) (Chapin et al. 2011) and, therefore, the signal generated from the probe region is not affected by changes in the thickness to the same extent seen with the fluorophore loading of the code.

The ability to incorporate magnetic materials in both code and probe regions provides a significant amount of versatility, which is especially useful in multiplex assays that require efficient use of particle area. For example, with the methods presented here, code regions can have two simultaneous functionalities (identifying the particle and responding to external magnetic fields), and probe regions can also have two functionalities (embedding DNA probe molecules and responding to magnetic fields). This is in contrast to previously developed methods, which required a separate patch on the gel for the immobilization of magnetic material. Combining functionalities with the synthesis reported here preserves more of the particle for encoding and/or biomolecule capture.

3.3 Patterning of magnetic microparticles using microwells

After demonstrating that the particles maintain functionality for biological assays, we developed a means of arraying the particles in small-volume microwells. Magnetic barcoded particles were efficiently manipulated into microwell chambers using hand magnets. These magnets were able to precisely rotate and translate magnetic particles; the magnetic regions of the particles align with the magnetic field to achieve the most energetically favorable configuration. The hand magnet was rotated to align the

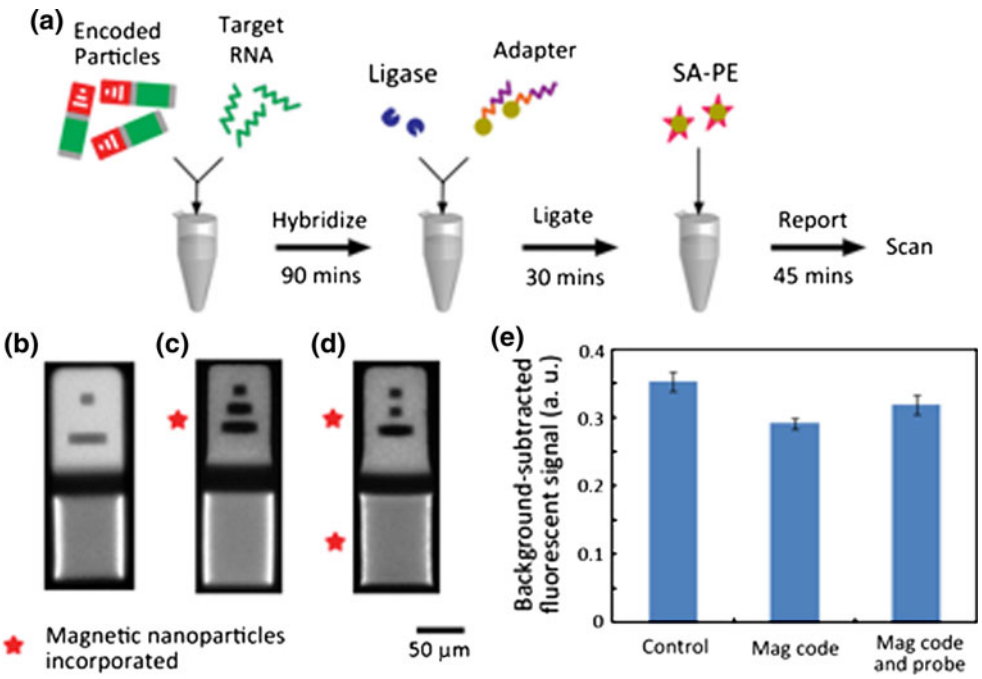

Fig. 2 miRNA detection using magnetic barcode particles after high-pH rinsing. **a** Schematic overview of the miRNA assay. **b** Fluorescent images of control particle with no magnetic material (code 103) **c**, a particle with a magnetic code (code 123) **d**, and a particle with magnetic code and magnetic probe (code 113), all shown after a miRNA assay. **e** Fluorescent signal from miRNA detection after scanning in a flow-through device. The *error bars* represent intra-run standard deviation

particles with the x-axis, as shown in Fig. 3. For translation of the particles into the microwells, we tilted the magnet 45° downward to direct particles along the x-axis and also into the wells. If the magnet does not pull the particles downward, the particles pass by the wells rather than fall into them. As shown in Fig. 3b, we were able to occupy all wells with magnetic particles. As it is difficult to move many particles in the desired direction simultaneously, approximately five particles were dropped on the surface of PDMS at a time and the filling process was repeated to occupy all the wells. As shown in Fig. 3b, we used two types of particles, which were sequentially loaded into wells. These particles were not distributed randomly, as the particles initially dropped were located in the closest wells. If a random distribution is important for certain applications, the particle types may be mixed prior to filling.

We investigated the statistics of hydrogel particle occupancy as shown in Fig. 3c. Non-magnetic particles can only be manipulated randomly with agitation, a process which is largely inefficient and imprecise. Therefore, more than half of the wells were not filled with non-magnetic particles, while most wells were filled with magnetic particles. We selected wells with a depth of 113 μm to prevent particles (depth of ~35 μm) from being swept out during rinse steps and to provide sufficient room for the loading of biological sample fluids or cells during potential biomolecule analysis experiments. Because of this depth, more than two particles can be placed in one well. However, we were able to manipulate the magnetic particles before they settled in order to avoid the issue of double occupancy.

The deposition of hydrogel particles in patterned microwells using external magnetic forces could be very beneficial for high-throughput or high-sensitivity applications as each microwell can act as an isolated reaction chamber. To utilize microwells for reactions with multiple processing steps, it is necessary to retain the particles within the wells while solutions are exchanged. It is common practice to cover microwells with a glass substrate during reaction/incubation (Ogunniyi et al. 2009) to prevent fluid communication between wells and evaporation of liquid. When removing such a glass containment substrate from our well setup, it was observed that non-magnetic particles could easily be pulled out of the wells and adsorbed onto the glass surface due to strong suction forces. This issue can be overcome by using magnetic particles, which can be immobilized at the bottom of the wells by applying a downward magnetic force. This can be accomplished by simply placing hand magnets underneath the wells.

3.4 Selective collection of individual particles using magnetic tweezers

It is also possible to collect hydrogel particles from selective microwells for relocation, further analysis, or discarding. We investigated selective manipulation of individual magnetic particles using magnetic tweezers. As shown in Fig. 4c, d, two types of particles (code 223 and 103) were used. We used magnetic tweezers to successfully remove only the particles with non-magnetic code (103) from the microwell array. We applied a lower current to the

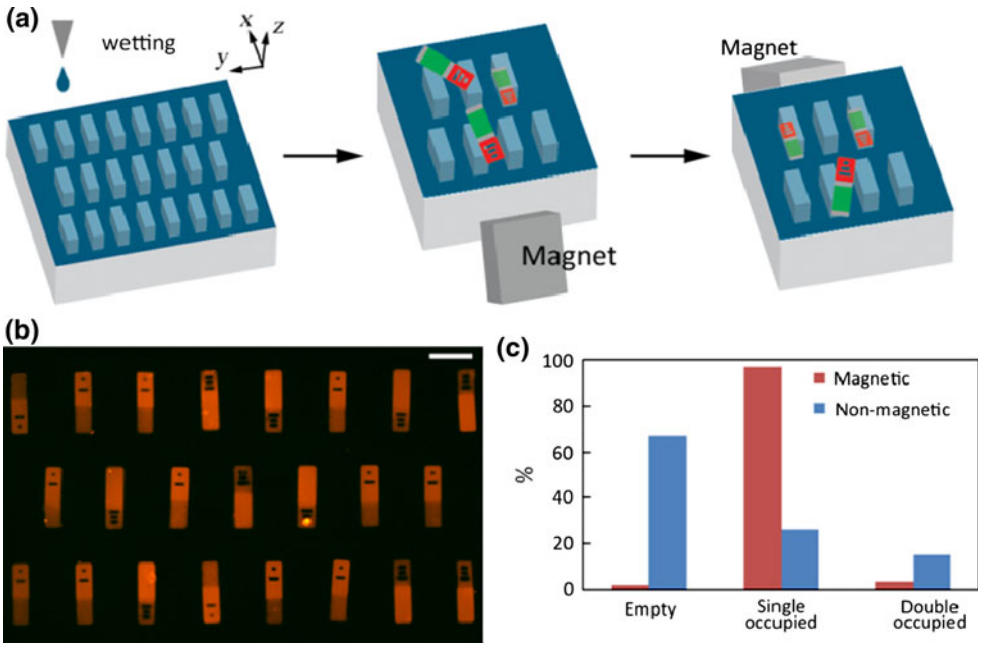

Fig. 3 Patterning of the magnetic barcode particles in microwells using a hand magnet. **a** Schematic description showing patterned substrate with subsequent addition and manipulation of magnetic particles into microwells. **b** Fluorescent images of microwells occupied with the two types of magnetic particles. The *scale bar* is 200 μm. **c** Statistics of well occupancy with magnetic (*red*) and non-magnetic (*blue*) barcoded particles (color figure online)

magnetic tweezer than in our previous work (Rich et al. 2011), to provide better tweezing resolution. A current of $I = 0.15$ A provided a strong enough force to attract targeted particles without disturbing other particles nearby. Also, the magnetic tweezer was able to pick up multiple particles, one at a time, enabling a more efficient collection. This is advantageous because one does not need to oscillate the applied current every collection to de-magnetize the magnetic tweezer, which exhibits magnetic hysteresis. The maximum number of particles collected without turning the tweezer off was 43. These proof-of-concept experiments show that particles can be collected effectively using a magnetic tweezer with precise control over single particles. Currently, this manual control might not be the most efficient way of particle collections, but it can be dramatically improved with process automation.

To estimate the magnetic force we apply to the composite gel microparticles, we first calibrate the magnetic tweezer by measuring the response of dispersed magnetic beads suspended in solution (not in a microgel). With our experimental setup, only the horizontal forces can be measured, although the collection of barcoded particles was based on forces in the vertical direction. Thus, for a more accurate measurement, we rotated the tweezer 90°. Figure 4b shows the velocity averaged over 20 beads as a function of distance from the tip of the magnetic tweezer. The velocity of the beads increased as they approached the tip, where the largest gradient existed in the magnetic field. Since the magnetic beads are spherical, the drag force can be calculated from Stokes' law,

$$F_{\text{drag}} = -6\pi\mu a U \tag{1}$$

where μ is the dynamic viscosity of the dispersed medium, a is the radius of the bead, and U is the bead velocity. Assuming that inertia is negligible, the sum of the magnetic force and the drag force is zero ($F_{\text{mag}} = -F_{\text{drag}}$). As the distance from the barcoded particles to the tip of the magnetic tweezer was $\sim$150 μm for particle collection, we obtained the velocity of the magnetic beads at the same distance, finding the average to be 1.9 μm/s. Using Eq. (1), we calculated the magnetic force exerted on one magnetic bead to have a value of 1.2×10^{-3} nN. We note that the value is smaller than that found in our previous work (Rich et al. 2011) due to the smaller size (and hence volume) of magnetic beads used here. To calculate the magnetic force exerted on the gel microparticles, we assumed that all magnetic beads embedded within the hydrogel experienced the same force. We multiplied an estimated number of

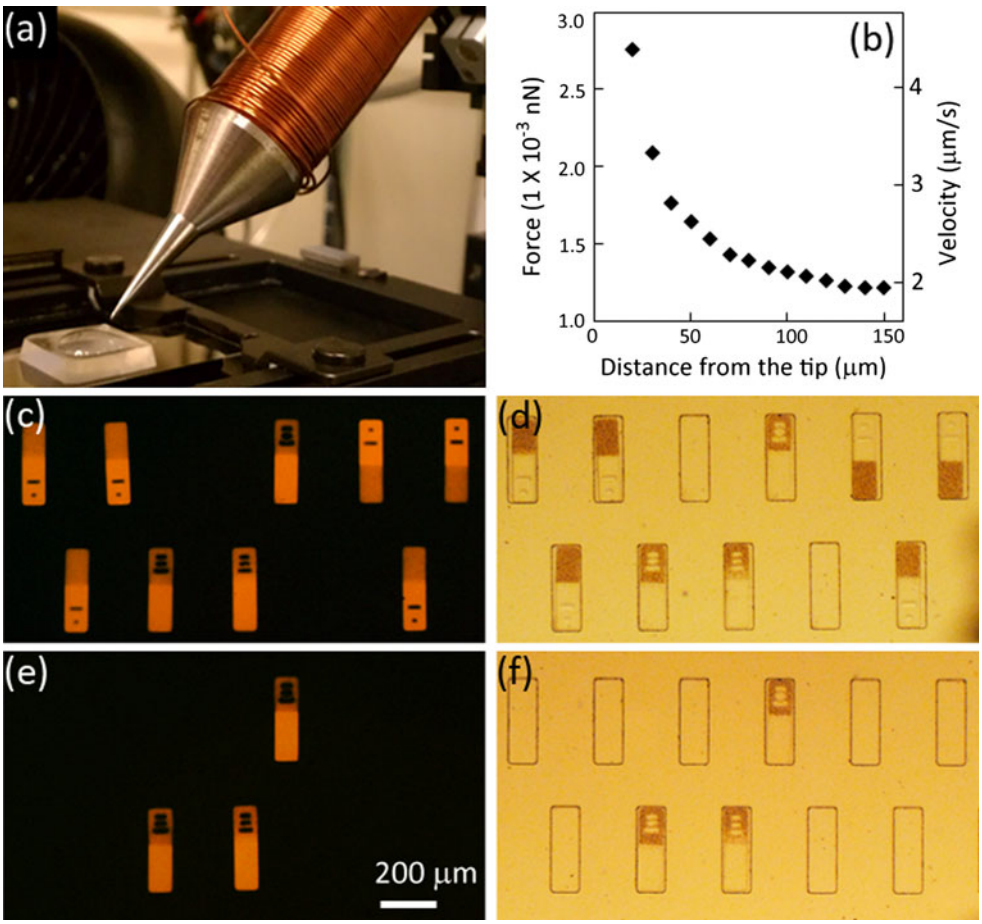

Fig. 4 Selective collection of magnetic particles using a magnetic tweezer. **a** The magnetic tweezer set up on the microscope stage. The tip was dipped in the solution when current was sent through the coil. **b** Average magnetic force exerted on one magnetic bead and average velocity as a function of distance from the tweezer tip. **c** Fluorescent image of microwells filled with two types of particles (distinguished by codes 223 and 103) with corresponding *bright field image* (**d**). **e** Fluorescent image of microwells shown in **c** after removing particles with code 103 using the magnetic tweezer. **f** Bright field image of **e**

magnetic beads in microparticles by the force exerted on a single bead, resulting in a total magnetic force on one barcoded particle of ~ 22 nN. The magnetic force calculated represents the upper bound, as not all beads are 150 μm from the tip. There are two more forces related to magnetic particle collection: gravitational and buoyancy forces. For simplicity, we defined F_g as the summation of both. Using an estimated density of barcoded particle ($\rho_p = 1.05$ mg/ml) and a density of suspended solution ($\rho_s = 0.998$ mg/ml), F_g was calculated with the following equation

$$F_g = g(\rho_p - \rho_s)V \quad (2)$$

where g is the gravitational acceleration and V is the volume of particles. The ratio between the magnetic to gravitational force exerted on a particle (F_{mag}/F_g) was 83. We note that this is the initial value, as the magnetic force (Fig. 4b) increases as particles approach the tip. It is possible that larger forces are needed for manipulation in some cases; for example, recovery from adherent surfaces. In this case, the spaces between wells can be designed more carefully, to accommodate the force required to manipulate individual particles without disrupting neighboring particles.

4 Conclusion

We developed a new technique to prepare and manipulate magnetic hydrogel particles, using external magnetic forces to arrange them in microwells. First, we demonstrated a modified synthesis process to remove magnetic debris from magnetic barcoded particles without losing the functionality of miRNA detection. We increased the versatility significantly by enabling dual functionalities in each particle region. Although the high-pH rinse used to remove debris can potentially damage biomolecules embedded in the particles (e.g., antibodies), one can use generic coupling chemistries, such as carboxyl groups, for post-synthesis particle functionalization. We also showed that the magnetic particles could be efficiently manipulated to occupy substrate-patterned microwells for use in small-volume analysis procedures. Furthermore, we selectively collected individual magnetic particles from the wells using a magnetic tweezer. The combination of encoded hydrogel particles with patterned substrates can enable high-throughput analysis of small-volume multiplexed bioassays, chemical reactions, or single-cell analysis. The ability to manipulate individual particles with magnetic fields can bring great flexibility for sequential processing or building of complex multi-dimensional hydrogel structures.

Acknowledgments This work was supported by Singapore-MIT Alliance and NSF grants DMR-100614 and DMR-1006147.

References

Appleyard DC, Chapin SC, Doyle PS (2011) Multiplexed protein quantification with barcoded hydrogel microparticles. Anal Chem 83(1):193–199

Bong KW, Chapin SC, Doyle PS (2010) Magnetic barcoded hydrogel microparticles for multiplexed detection. Langmuir 26(11): 8008–8014

Bong KW, Chapin SC, Pregibon DC, Baah D, Floyd-Smith TM, Doyle PS (2011) Compressed-air flow control system. Lab Chip 11(4):743–747

Bucak S, Jones DA, Laibinis PE, Hatton TA (2003) Protein separations using colloidal magnetic nanoparticles. Biotechnol Progr 19(2):477–484

Chapin SC, Pregibon DC, Doyle PS (2009) High-throughput flow alignment of barcoded hydrogel microparticles. Lab Chip 9(21):3100–3109

Chapin SC, Appleyard DC, Pregibon DC, Doyle PS (2011) Rapid microRNA profiling on encoded gel microparticles. Angew Chem Int Ed 50(10):2289–2293

Cheng NS (2008) Formula for the viscosity of a glycerol–water mixture. Ind Eng Chem Res 47(9):3285–3288

Choi JW, Oh KW, Thomas JH, Heineman WR, Halsall HB, Nevin JH, Helmicki AJ, Henderson HT, Ahn CH (2001) An integrated microfluidic biochemical detection system for protein analysis with magnetic bead-based sampling capabilities. Lab Chip 2(1): 27–30

Doyle PS, Bibette J, Bancaud A, Viovy JL (2002) Self-assembled magnetic matrices for DNA separation chips. Science 295 (5563):2237

Dyab AKF, Ozmen M, Ersoz M, Paunov VN (2009) Fabrication of novel anisotropic magnetic microparticles. J Mater Chem 19(21): 3475–3481

Fessenden RJ, Fessenden JS, Logue MW (1998) Organic Chemistry, 6th edn. Brooks/Cole Publishing Co, Pacific Grove

Gunn NM, Chang R, Westerhof T, Li GP, Bachman M, Nelson EL (2010) Ferromagnetic micropallets for magnetic capture of single adherent cells. Langmuir 26(22):17703–17711

Jung JH, Kim G-Y, Seo TS (2011) An integrated passive micromixer-magnetic separation-capillary electrophoresis microdevice for rapid and multiplex pathogen detection at the single-cell level. Lab Chip 11(20):3465–3470

Kim SH, Sim JY, Lim JM, Yang SM (2010) Magnetoresponsive microparticles with nanoscopic surface structures for remote-controlled locomotion. Angew Chem Int Ed 49(22):3786–3790

Lammerding J (2004) Quantitative Analysis of Subcellular Biomechanics and Mechanotransduction. Massachusetts Institute of Technology

Lee H, Kim J, Kim H, Kwon S (2010) Colour-barcoded magnetic microparticles for multiplexed bioassays. Nat Mater 9(9): 745–749

Lindström S, Andersson-Svahn H (2010) Miniaturization of biological assays–overview on microwell devices for single-cell analyses. Biochim Biophys Acta (BBA)-General Subjects 1810 (3):308–316

Love JC, Ronan JL, Grotenbreg GM, van der Veen AG, Ploegh HL (2006) A microengraving method for rapid selection of single cells producing antigen-specific antibodies. Nat Biotechnol 24(6):703–707

Miltenyi S, Müller W, Weichel W, Radbruch A (1990) High gradient magnetic cell separation with MACS. Cytometry 11(2):231–238
Mornet S, Vasseur S, Grasset F, Duguet E (2004) Magnetic nanoparticle design for medical diagnosis and therapy. J Mater Chem 14(14):2161–2175
Ogunniyi AO, Story CM, Papa E, Guillen E, Love JC (2009) Screening individual hybridomas by microengraving to discover monoclonal antibodies. Nat Protoc 4(5):767–782
Pamme N, Manz A (2004) On-chip free-flow magnetophoresis: continuous flow separation of magnetic particles and agglomerates. Anal Chem 76(24):7250–7256
Pankhurst QA, Connolly J, Jones SK, Dobson J (2003) Applications of magnetic nanoparticles in biomedicine. J Phys D Appl Phys 36(13):R167–R181
Peyman SA, Iles A, Pamme N (2009) Mobile magnetic particles as solid-supports for rapid surface-based bioanalysis in continuous flow. Lab Chip 9(21):3110–3117
Pregibon DC, Toner M, Doyle PS (2007) Multifunctional encoded particles for high-throughput biomolecule analysis. Science 315(5817):1393–1396
Rich JP, Lammerding J, McKinley GH, Doyle PS (2011) Nonlinear microrheology of an aging, yield stress fluid using magnetic tweezers. Soft Matter 7(21):9933–9943
Saliba A-E, Saias L, Psychari E, Minc N, Simon D, Bidard F-C, Mathiot C, Pierga J-Y, Fraisier V, Salamero J, Saada V, Farace F, Vielh P, Malaquin L, Viovy J-L (2010) Microfluidic sorting and multimodal typing of cancer cells in self-assembled magnetic arrays. Proc Nat Acad Sci USA 107(33):14524–14529
Seiffert S, Romanowsky MB, Weitz DA (2010) Janus microgels produced from functional precursor polymers. Langmuir 26(18): 14842–14847
Slovakova M, Minc N, Bilkova Z, Smadja C, Faigle W, Futterer C, Taverna M, Viovy JL (2005) Use of self assembled magnetic beads for on-chip protein digestion. Lab Chip 5(9):935–942
Srinivas RL, Chapin SC, Doyle PS (2011) Aptamer functionalized microgel particles for protein detection. Anal Chem 83:9138–9145
Stevens PD, Fan J, Gardimalla HMR, Yen M, Gao Y (2005) Superparamagnetic nanoparticle-supported catalysis of Suzuki cross-coupling reactions. Org Lett 7(11):2085–2088
Suh SK, Bong KW, Hatton TA, Doyle PS (2011) Using stop-flow lithography to produce opaque microparticles: synthesis and modeling. Langmuir 27(22):13813–13819
Xu F, Wu CM, Rengarajan V, Finley TD, Keles HO, Sung Y, Li B, Gurkan UA, Demirci U (2011) Three-dimensional magnetic assembly of microscale hydrogels. Adv Mater 23(37):4254–4260
Yin SN, Wang CF, Yu ZY, Wang J, Liu SS, Chen S (2011) Versatile bifunctional magnetic-fluorescent responsive Janus supraballs towards the flexible bead display. Adv Mater 23(26):2915–2919
Yuet KP, Hwang DK, Haghgooie R, Doyle PS (2010) Multifunctional superparamagnetic Janus particles. Langmuir 26(6):4281–4287